

Ontogenetic effects on locomotory gaits in nymphs of *Baetis tricaudatus* Dodds (Ephemeroptera:Baetidae)

TRACY N. KUTASH AND DOUGLAS A. CRAIG¹

Department of Biological Sciences, University of Alberta, Edmonton, Alberta, Canada T6G 2E9

Abstract. The locomotory behavior of *Baetis tricaudatus* Dodds nymphs was examined by placing individuals of various lengths in a still-water tank and recording movement sequences using high-speed cinematography and video. Gait of small nymphs (≤ 3.0 mm) differed from that of larger nymphs (≥ 4.0 mm). Small nymphs combined dorso–ventral oscillations of the abdomen in addition to rowing with their legs, whereas large nymphs used only abdominal oscillations for propulsion. Transition from rowing to swimming gait occurred when the nymphs were ca 3.5 mm long, at Reynolds numbers of 60–90. When viscous forces predominate, friction-based methods of locomotion (i.e., rowing) are most efficient, whereas propulsive methods (i.e., abdominal undulations involving vortices—swimming) are more effective when inertial forces prevail. Small *B. tricaudatus* nymphs row because viscous forces do not allow propulsive mechanisms, and the use of leg orientation minimizes drag of the recovery stroke relative to that of the power stroke. Average speed increased linearly with body length in small nymphs, but exponentially in large nymphs. The shift from linear to exponential increase in speed occurred within the same range of body lengths as did change in gait. Ontogenetic changes in gait and speed could be the mechanisms that regulate other size-dependent behaviors observed in *Baetis* spp., namely those involved with risk management and predator avoidance.

Key words: Ephemeroptera, *Baetis*, nymphs, gait, rowing, swimming, hydrodynamics, Reynolds number, size, behavior, predator avoidance.

Mayfly nymphs use a variety of primary and secondary defenses to avoid or escape predation, and the types of defensive actions taken by a nymph can be partly predicted by its external morphology. Baetid nymphs frequently respond to a predator by swimming, despite their initial response of decreased activity (Peckarsky 1980). Although streamlined mayfly nymphs are frequently used in laboratory and field studies, details regarding their swimming behavior and performance are limited (but see Craig 1990). It is generally accepted, however, that streamlined nymphs are capable of rapid swimming (e.g., Needham and Lloyd 1916, Hynes 1970, Nachigall 1974).

Understanding locomotory performance of an organism is important because outcomes of predator–prey interactions are influenced by the physical capabilities of the participants (Webb 1986). Locomotory performance of an aquatic organism is affected by both abiotic conditions (i.e., temperature, flow velocity, viscosity) and structure of the animal (i.e., size, shape, muscle arrangement). Sufficiently large increases in size, speed, or body shape may result in an alteration of the immediate hydrodynamic regime

an animal occupies. For example, because of their small size, larval fish occupy a regime very different from that of the adults (e.g., Batty 1981, 1984, Webb and Weihs 1986). Changes in the hydrodynamic regime also occur as a consequence of increased swimming speeds. In fish, for example, the change is characterized by a transition from labriform to carangiform swimming modes (Archer and Johnston 1989).

A general indicator of how a fluid will flow upon encountering a solid is given by the Reynolds number (Re), which broadly defines the ratio of viscous to inertial forces acting on the organism. A gradual change in an animals' hydrodynamic regime, and hence the type of locomotory mechanism that it can use, occurs between Re 20 to 200 (Webb and Weihs 1986). This range defines a hydrodynamic transition zone where flow characteristics change from one where viscous forces dominate to one where inertial forces prevail (Webb and Weihs 1986). When $Re << 1$, viscous forces predominate over inertial ones, but viscous forces are still significant up to $Re = 10$ and possibly $Re = 30$ (Weihs 1980).

To adjust to ontogenetic changes such as growth, which alter the hydrodynamic regime, an aquatic animal should show changes in lo-

¹ To whom correspondence should be addressed.
E-mail: d.craig@ualberta.ca

comotory gait (*sensu* Webb 1994). It should use friction-based locomotory methods such as rowing at low Re , and propulsive mechanisms such as undulatory swimming at high Re (e.g., Hunter 1972, Batty 1981, 1984, Daniel and Webb 1987). Increases in length or change in body shape during ontogeny will alter the Re , and hence the nature of flow patterns and drag forces acting on the animal. This change is well understood during ontogeny of larval fish, in which spherical body shape of newly hatched larvae precludes high Re , but later absorption of the yolk sack allows the larva to rapidly switch to higher Re (Webb and Weihs 1986). However, even early larvae can undergo sprint (= burst) activity to achieve $Re >> 200$. Aquatic insect nymphs may not display optimal drag-minimizing morphologies, nor will they experience equal flow conditions throughout all instars, assuming the various instars occupy the same microhabitat. Small nymphs, with a high surface area-to-volume ratio, will experience relatively more skin friction than large ones, whereas large nymphs are more intensely affected by inertial-based drag forces. Statzner (1988) concluded that "evolution compromises between life at low and high Re " and therefore "the shape of a benthic macroinvertebrate is not adapted in such a way that drag is minimized at a certain Re ". However, these assertions ignore changes in an organisms' locomotory behavior that occur during ontogeny.

In southern Alberta, *Baetis tricaudatus* Dodds nymphs commonly have 2 overlapping generations with 1 small and 1 large size class occurring together in the same microhabitat (Culp and Scrimgeour 1993). A difference in locomotory behavior between these 2 size classes of nymphs should be expected purely on principles of fluid dynamics. Indeed, Behan (1997) has shown from 1st principles that the 1st eddy or vortex formed in flowing water occurs at $Re \approx 100$. In general, below this value, viscous forces predominate and friction-based methods of locomotion are used; above $Re \approx 100$, propulsive mechanisms that use vortices for lift and thrust are used. Our study further examines the relationship between locomotion and hydrodynamic environment by analyzing various aspects of locomotory gait in 2 size classes of *B. tricaudatus* nymphs. We show that the gait of these small nymphs is highly dependent on their hydrodynamic environment and that ontogenetic changes

in gait have implications for predator-prey interactions.

Methods

Experimental animals

Baetis tricaudatus nymphs were collected from Stauffer Creek, 10 km north of Caroline, south-central Alberta, Canada. Nymphs were brought to the laboratory and placed in aquaria with controlled ambient temperatures of 13°C and a 14 h:10 h light:dark cycle. Large stones were positioned in the center of aquaria and air stones were placed in 1 corner to generate a current. Long-term mortality was high, so all experiments were conducted within 1 mo of collecting.

Filming

A still-water system was used to simplify experiments so that effects of water flow would not have to be considered. Furthermore, nymphs in a flowing system would have been carried downstream as they entered the water column. An experimental tank constructed of 1-mm thick Plexiglas® with interior dimensions 65 mm H × 25 mm W × 75 mm L was filled with 100 mL of water taken from the rearing tank. Initial temperature in the experimental tank was ca 13°C, but temperature rose slightly during the course of filming. A light diffuser placed behind the tank was back-lit with 2 Wild® 120 W lights that were positioned to illuminate the entire area of the experimental tank.

Prior to recording locomotory sequences, ~10 nymphs of various sizes were placed in the experimental tanks and allowed to acclimate for at least 10 min. A precision ruler placed in the experimental tank was filmed for calibration before sequences were recorded. Nymphs were allowed to move spontaneously, but were occasionally stimulated with a metal probe to induce locomotion.

Gait sequences were recorded using both high-speed cinematography and high-speed video. For high-speed cinematography, a Super-8 mm, high-speed camera (Cine-8 Model V, Mekel Engineering Co., Covina, California) fitted with a Nikon, Micro-NIKKOR®, 55-mm lens, was used to record nymphs at 250 frames per second (f/s, = 0.004 s between frames) us-

ing Kodak, Tri-X® reversal film (type 7278). Observations recorded on high-speed cine film were projected at ca 500 \times magnification using a stop-motion projector (Lafayette Analyzer Model 00927, Lafayette Instrument Co. Lafayette, Indiana). A high-speed video camera (Kodak Ektapro® 1000, Motion Analyzer) recording at 1000 f/s was also used for some sequences. Data were then downloaded at 30 f/s to a Panasonic VCR. (Model AG6200®) and measurements were taken from images on a Sony Trinitron®, super-fine pitch monitor (Model CVM-1270). A total of 62 larvae were observed for gait; of these, 38 met the criteria (below) for detailed analysis.

Analyses

Average speed.—Swimming sequences recorded from high-speed cinematography and high-speed video were pooled to increase the number of observations used to determine the relationship between length and average swimming speed/*Re*. Although swimming behavior and length were recorded for all nymphs, only film sequences where the nymph remained in the plane of focus were chosen for average speed analysis. A reference mark was placed on the 1st projected image at the base of the antennae, and the film was advanced until the sequence was completed. Another reference mark was placed on the final image of the series, creating a path depicting the average displacement of the nymph. If the path swum was not linear, marks were placed on suitable images when a change in direction occurred. Elapsed time was monitored using the frame counter on the projector or video screen. Distance swum was measured from the tracing using a video camera (Hitachi® VK-C350 fitted with a Nikon® 55-mm lens) connected to a Macintosh IIfx computer, which used the image analysis program, Image© 1.41 (National Institute of Health, Research Services Branch, National Institute of Medicine and Health, Bethesda, Maryland).

Displacement data were used to calculate the average speed (U_{av}) using the equation:

$$U_{av} = \frac{\Delta d}{\Delta t}$$

where d = distance swum and t = time elapsed.

Instantaneous speed and acceleration.—These values were determined from sequences taken

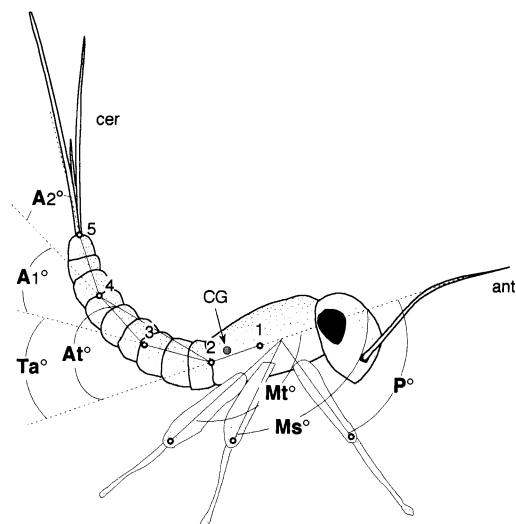


FIG. 1. Schematic lateral view of a *Baetis tricaudatus* nymph, showing positions of reference points for determination of abdominal flexion and leg rotation angles. At° = average abdominal flexion; Ta° = thoracic-abdominal flexion; $A1^\circ$ = 1/3 length of abdomen; $A2^\circ$ = 2/3 length of abdomen; P° = pro-, Ms° = meso-, and Mt° = metathoracic leg angles; ant = antennae; cer = cerci; CG = center of gravity. Line extrapolated from points 1 and 2 represents the longitudinal body axis.

from high-speed cine films, as described for the average speed. Only nymphs that remained in the plane of focus were selected for sequential frame analysis. A reference mark located at the center of gravity (CG, ca 0.4 \times the length of nymph from the head, cerci not included) was placed on each image in a sequence to determine the path of movement because the CG is the point through which the sum of all forces act on a body (Fig. 1). Nymphal length was measured from the front of the head to the tip of the abdomen. Distances between consecutive CG points on the drawings were measured using Image 1.41. Data for calculating speed and acceleration were smoothed using a 3-point polynomial smoothing routine. Instantaneous speed (U) was calculated the same way as average speed ($= \Delta d / \Delta t$); instantaneous acceleration was determined using the formula:

$$a = \frac{\Delta U}{\Delta t}$$

where U = instantaneous speed and t = time elapsed.

Abdominal angles.—To determine the relationship between abdominal undulation and speed, 5 reference points were placed on the tracing of each frame image: 1) center of the thorax, 2) the junction between the thorax and abdomen (near the CG), 3) 1/3 the length of the abdomen from the thorax, 4) 2/3 the length of the abdomen from the thorax, and 5) the tip of the abdomen (Fig. 1). All reference points were positioned mid-way between the dorsal and ventral surfaces of the nymph. A line through points 1 and 2 represented the long axis of the body. The points along the abdomen were selected because most of the articulation occurred around those sections. The following angles were measured in the analysis: Ta° , the angle created through the intersection of lines 1–2 and 2–3; $A1^\circ$, the angle at the intersection of lines 2–3 and 3–4; and $A2^\circ$, the angle at the intersection of lines 3–4 and 4–5 (Fig. 1). Another angle (At°) created through the intersection of lines 1–2 and 2–4 was used to describe the overall abdominal position during a swimming cycle. Resulting angles were measured using Image 1.41.

Leg angles.—Tracings of the nymphs showing leg positions were made for each image in a sequence. Points were placed at the distal end of the femur of each leg. A line was drawn through the long axis of the femur to intersect with the long axis of the body (line 1–2), and the angle of leg rotation was taken between the femoral and the body axis (Fig. 1). These angles (P° , Ms° , and Mt°) were measured and analyzed as for abdominal angles. Because of the poor resolution of the film, the proximal leg segments could not be seen; therefore, leg lengths were measured from the points at which they began to project from the body to the distal end of the tibia. The meso- and metathoracic pairs of legs, although somewhat flexed during swimming, were treated as straight and rigid structures. Average leg and abdominal angles are given as mean ± 1 SE.

Hydrodynamic equations.—Reynolds number was calculated for all sequences analyzed and is defined as: $Re = LU/\nu$ where L = greatest length of a body parallel to the flow (excluding cerci), U = relative speed at the fluid-solid interface (speed of the nymph), and ν = kinematic viscosity ($\nu = 1.1 \times 10^{-6} \text{ m}^2/\text{s}$, freshwater at 13°C), which is constant for a particular fluid at a given temperature. The cerci were not included in the length measurement since they nor-

mally were splayed laterally and not in the plane of focus.

Results

*Swimming gait in small *B. tricaudatus* nymphs ($\leq 3.0 \text{ mm}$)*

Behavior.—Small *B. tricaudatus* nymphs moved by flexion of the abdomen in a dorso–ventral plane in conjunction with synchronized leg rowing movements (Figs 2, 3). As the abdomen flexed, the head and thorax also rotated in a dorso–ventral plane. This manner of swimming was consistent for all nymphs $\leq 3.0 \text{ mm}$ long. Although some nymphs between 3.3–3.7 mm also rowed, gait within this size range depended on the individual and not on length. None of the nymphs displayed lateral flexion of the abdomen.

For a nymph 1.3 mm long, the power stroke began with the abdomen maximally flexed (dorsally) and legs extended ventrally and somewhat laterally away from the body with a ca 60° angle between the pro- and metathoracic legs (Fig. 2a). When the abdomen was thrust downwards, the prothoracic legs continued to be brought forward while the meso- and metathoracic legs were brought backwards, which increased the angle between the pro- and metathoracic legs (Fig. 2b–d). The greatest angle between the pro- and metathoracic legs occurred about halfway through the deflexion of the abdomen as it approached its most linear position (Fig. 2e, f). Following this, the prothoracic legs retracted and the meso- and metathoracic legs started to move anteriorly. As the legs were drawn closer together, the abdomen was deflected further ventrally (Fig. 2f–j). At the same time the head and thorax were also tilted ventrally. Power strokes were completed when the abdomen was fully deflexed ventrally. With the onset of abdominal recovery, all leg pairs were synchronously moved anteriorly in a slightly flexed position (Fig. 2k–m) and continued to be drawn closer together. When the abdomen started to flex dorsally once again, the legs began to extend outwards and the angles between them increased (Fig. 2n–r).

The legs also extended laterally from the body during rowing. For example, in a nymph 3.4 mm long, the meso- and metathoracic legs were the 1st to move posteriorly during the

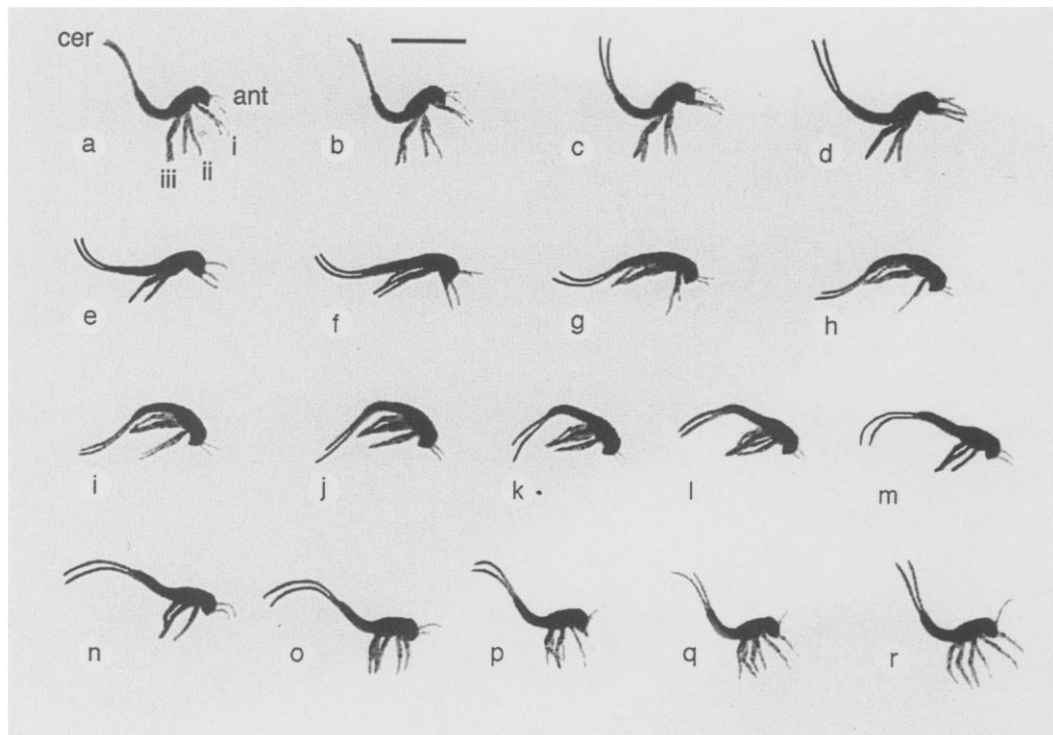


FIG. 2. Lateral view from a high-speed cine film sequence of the rowing cycle of a *Baetis tricaudatus* nymph (1.3 mm length), showing abdominal flexion and leg positions. Time elapsed between images = 0.004 s. i, ii, iii = pro-, meso-, and metathoracic legs; ant = antennae; cer = cerci. Scale bar = 1 mm.

power stroke (Fig. 3a–c). When the body was in the most linear configuration, the prothoracic pair of legs were moved posteriorly (Fig. 3d). As the abdomen approached maximum deflection, the legs were brought close to the body (Fig. 3e–h). As a result, the lateral projection of legs was at a minimum. At the onset of the recovery stroke, all legs synchronously moved anteriorly until the body reached a linear configuration again (Fig. 2n), at which time legs simultaneously began to extend slightly laterally (Fig. 3i–l). When the abdomen began to flex dorsally, the legs extended outwards (Fig. 3m–p). Movement of the thoracic legs resembled the arm motions of a swimmer doing the breast stroke, where the arms are 1st extended anteriorly and then drawn back postero-laterally for the power stroke (protraction), but are kept close to the body with virtually no lateral projection during the recovery stroke (retraction).

A typical rowing sequence consisted of a short burst of activity (usually fewer than 5 cycles) into the water column. Once in the column,

nymphs generally ceased movement and assumed a splayed position with their legs extended ventro-laterally with the abdomen flexed. This position was maintained until the nymphs either sank to the bottom of the tank, or resumed a series of rowing cycles.

Abdominal oscillations.—Flexion around At° , Ta° , $A1^\circ$ and $A2^\circ$ (Fig. 1) varied depending on the length of nymph. For a nymph measuring 1.3 mm, the greatest angle of flexion occurred around At° ($74.2^\circ \pm 2.5^\circ$, mean ± 1 SE) followed by Ta° ($60.2^\circ \pm 2.9^\circ$), $A1^\circ$ ($40.1^\circ \pm 3.2^\circ$), and $A2^\circ$ ($19.2^\circ \pm 5.1^\circ$) (Fig. 4a). Deflection was greatest around $A2^\circ$ with $A1^\circ$ showing a slightly greater angle of deflection than Ta° . Total amplitude of flexion was highest around At° ($95.0^\circ \pm 5.5^\circ$) followed by Ta° ($74.9^\circ \pm 4.2^\circ$), and $A2^\circ$ ($63.8^\circ \pm 3.3^\circ$), and was lowest around $A1^\circ$ ($52.6^\circ \pm 1.6^\circ$). Synchronization of flexion and deflection angles indicated that the abdomen behaved as a semi-stiff plate and did not undulate.

Oscillation of the abdomen differed slightly in larger nymphs. For a nymph 2.0 mm long, high-

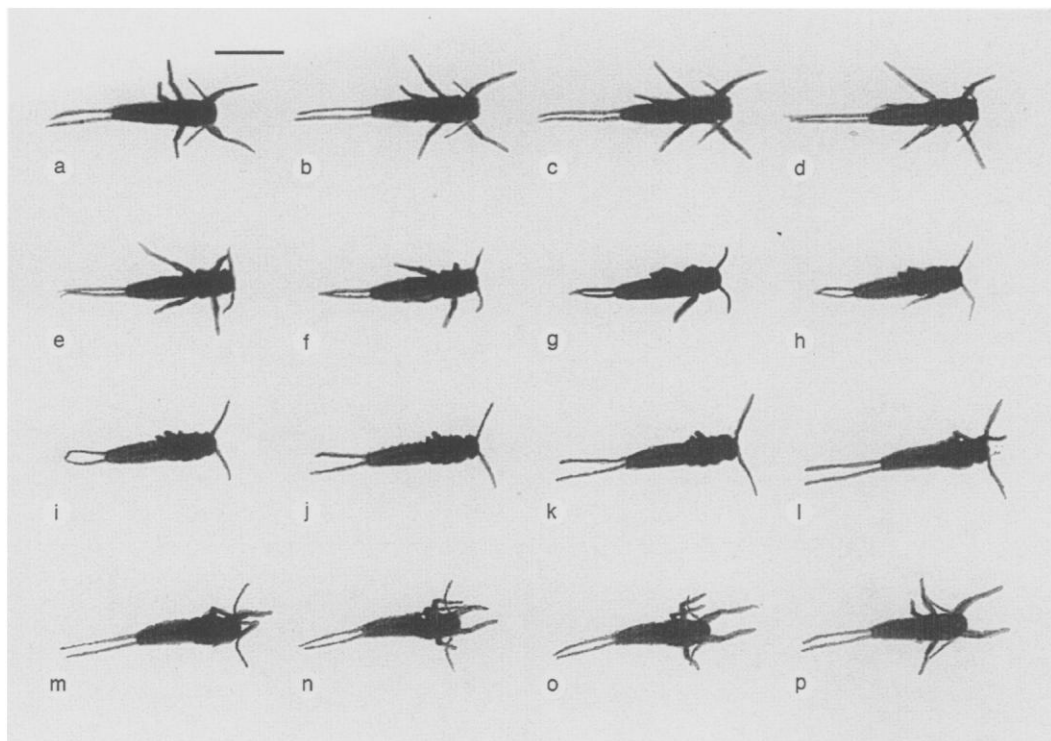


FIG. 3. Ventral view from a high-speed cine film sequence of the rowing cycle of a *Baetis tricaudatus* nymph (3.4 mm length), showing leg positions. Time elapsed between images = 0.004 s. Scale bar = 2 mm.

est flexion was around A1° (the middle 1/3 of the abdomen, $89.8^\circ \pm 6.0^\circ$), followed by that about the distal 1/3 (A2°); flexion about the segment nearest the thorax (Ta°) was lowest (Fig. 5). The greatest angle of deflexion occurred at the distal 1/3 of the abdomen (A2°) and the deflexion around Ta° and A1° were about equal. Amplitude of oscillation about A1° and A2° were $74.7^\circ \pm 2.5^\circ$ and $75.9^\circ \pm 2.8^\circ$, respectively, whereas the amplitude about the thoracic was $47.6^\circ \pm 1.7^\circ$. The period of oscillation of the 3 abdominal segments was slightly asynchronous, with the segment oscillating around Ta° always the 1st to complete a cycle, followed closely by the middle segment, and finally the distal segment, indicating that the abdomen was undulating slightly.

Leg rotation.—Rowing in *B. tricaudatus* followed a typical 3-2-1 metachronal pattern, although at most points during the cycle the prothoracic legs traveled in a direction opposite to that of the meso- and metathoracic legs, which tended to move synchronously (Figs 2, 3). When the angle between the prothoracic legs and the

long axis of the body was smallest, the angles between the meso- and metathoracic legs and the long axis were at the highest degree of rotation from the anterior. This position occurred just after the abdomen was thrust downwards upon the initiation of the power stroke. Of the 3 leg pairs, the prothoracic legs traveled through the largest angle ($62.2^\circ \pm 3.5^\circ$), followed by the metathoracic legs ($50.5^\circ \pm 4.8^\circ$), and the mesothoracic legs ($39.3^\circ \pm 4.3^\circ$) (Fig. 4b).

Average rowing speed.—Nymphs showed a linear increase in average speed with increased body length. Average swimming speed (U_{av}) and nymphal length (L) had the following relationship: $U_{av} = 6.4L + 2.9$ ($r^2 = 0.470$, $p = 0.0004$, $n = 22$). Since Re is dependent on speed, the relationship between length and Re was also linear: $Re = 22.1L - 16.8$ ($r^2 = 0.813$, $p = 0.0001$, $n = 22$).

Instantaneous rowing speeds and acceleration.—Eight small nymphs were analyzed for instantaneous rowing speed. Instantaneous speed fluctuated during the swimming cycle and depended on both abdominal and leg positions.

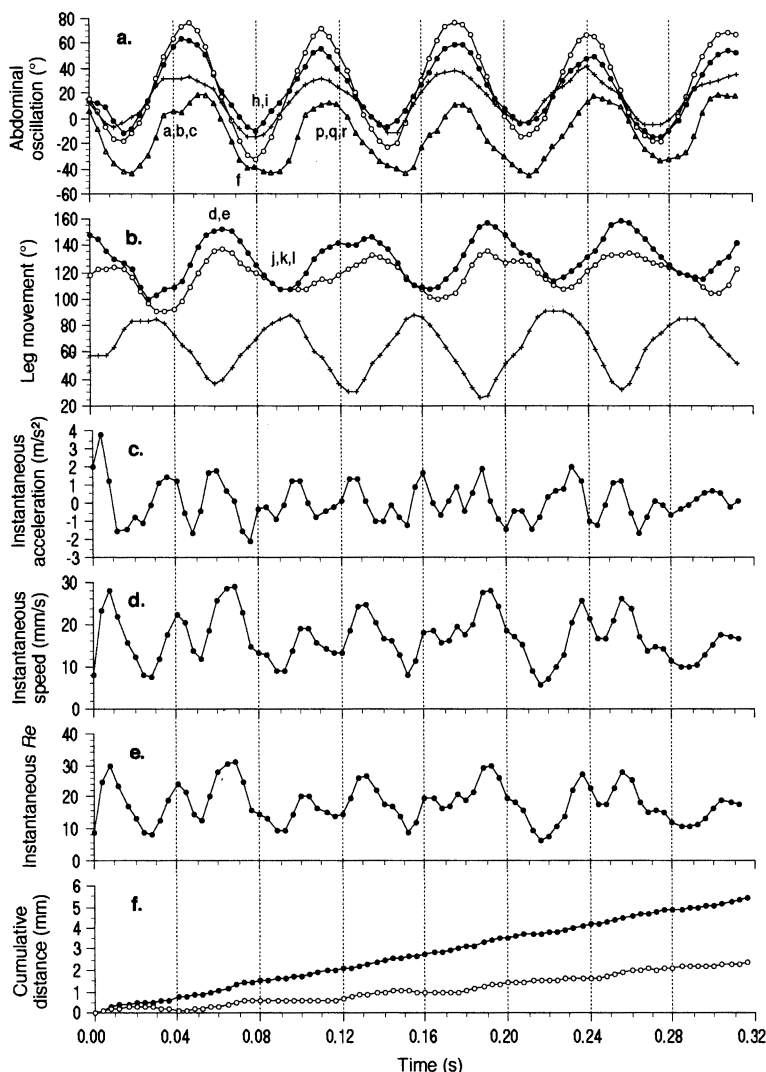


FIG. 4. Relationships among (a) angle of abdominal oscillation ($\circlearrowleft = At^\circ$, $\bullet = Ta^\circ$, $+ = A1^\circ$, $\triangle = A2^\circ$), (b) angle of leg movement ($+$ = pro-, \circlearrowleft = meso-, \bullet = metathoracic legs), (c) instantaneous acceleration, (d) instantaneous speed, (e) instantaneous Reynolds number (Re), and (f) cumulative distance (\bullet = total distance, \circlearrowleft = horizontal distance), during 5 rowing sequences in a *Baetis tricaudatus* nymph (1.3 mm long). Letters on (a) and (b) refer to film sequences in Figs 2 and 3, respectively.

Measurements taken from a 1.3 mm nymph showed that minimum rowing speeds (Fig. 4d) occurred when the abdomen was either maximally flexed or deflexed (Fig. 4a), at which time the nymph was nearing completion of either a power or recovery stroke of the legs (Fig. 4b). During a rowing cycle, there were 2 local maxima in speed and acceleration. The highest speed and acceleration during a cycle were reached during the power stroke when the ab-

domen approached its most linear position and the angle between the pro- and meta-thoracic legs was largest (Fig. 4a, b). The other maximum occurred following the onset of the recovery stroke when the abdomen was again approximately in a linear position and the pro- and meta-thoracic legs were closest together. Instantaneous Re (Fig. 4e) frequently fell to near 10 during a rowing cycle as the abdomen approached the highest degree of flexion or de-

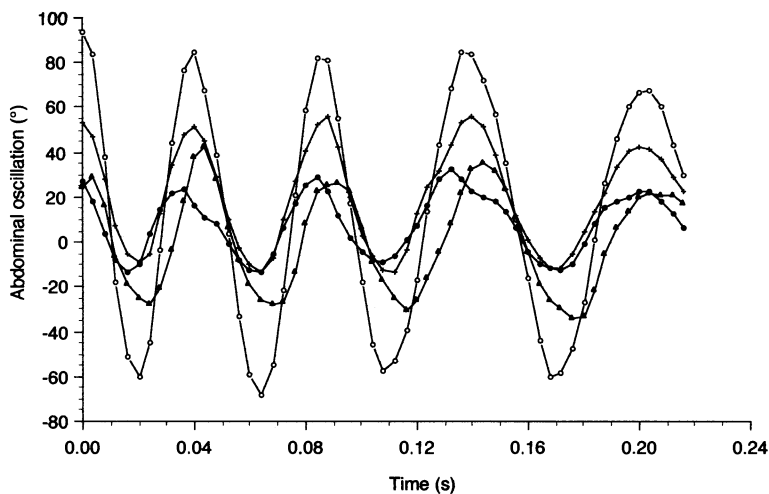


FIG. 5. Abdominal oscillation during locomotion in a *Baetis tricaudatus* nymph (2.0 mm long). ○ = At° , ● = Ta° , + = $A1^\circ$, △ = $A2^\circ$.

flexion and reached a maximum (ca 30) when the body was in the most linear configuration. Although the net motion of the body was forward, backward movement occurred during the recovery stroke (Fig. 4f), and produced a jerky motion as the nymph progressed.

Values taken from a 2.0 mm nymph (Fig. 5) showed that total amplitudes of abdominal oscillations were fairly constant, averaging $166.3^\circ \pm 3.5^\circ$. Although the amplitude remained constant, the mean angle of flexion was $89.8^\circ \pm 6.0^\circ$, whereas the mean angle of deflection was consistently lower ($68.2^\circ \pm 3.4^\circ$). Frequency (f) of oscillation gradually decreased with time, from 27.8 Hz in the 1st cycle to 15.6 Hz in the last cycle. This decrease in frequency was highly correlated with a reduction in average speed and had the following relationship: $U_{av} = 0.5f + 12.7$ ($r^2 = 1.0$, $p = 0.0001$, $n = 4$).

Swimming gait in large Baetis tricaudatus nymphs (≥ 4.0 mm)

Behavior.—Large nymphs swam only by oscillating the abdomen in a dorso-ventral plane; none displayed leg rowing. The power stroke of a 4.4 mm nymph was initiated when the abdomen was in the most highly flexed position (Fig. 6a). Prior to the onset of the power stroke, the speed was at a minimum (Fig. 7c). As the abdomen deflexed, speed and acceleration of the nymph increased and reached maxima when

body alignment was most linear (Figs 6d, 7a, b, c). The abdomen then continued ventrally (Fig. 6e, f, g) and the speed gradually declined (Fig. 7c), stopping when the abdomen reached maximum deflection. The power stroke for this nymph, which swam at an average speed of 49.8 mm/s, was completed in ~ 0.020 s. Recovery was initiated as the abdomen was thrust upward from the most ventral position (Fig. 6a). Maximum speed for the stroke was reached when the angle between the abdomen and the body approached 180° (Fig. 6g, h). The recovery stroke was completed in approximately the same time as the power stroke.

Abdominal oscillations.—For a nymph 4.4 mm long, the flexion around At° was initially highest, $A2^\circ$ was highest overall, followed by that of $A1^\circ$; Ta° was lowest (Fig. 7a). No segment consistently had the highest flexion for all cycles in a sequence. Total amplitude of oscillation about Ta° , $A1^\circ$, and $A2^\circ$ was $65.5^\circ \pm 7.3$, $72.9^\circ \pm 5.3$, and $66.9^\circ \pm 3.4$, respectively. The segment oscillating around Ta° was always the 1st to complete a cycle, followed by the middle and distal segments. Maximum abdominal flexion (measured about At°) was about double that of deflection for a power stroke and the corresponding recovery stroke in a swimming sequence. Oscillation of abdominal segments was distinctly asynchronous (Fig. 7a), indicating that the abdomen was undulating.

Although both frequency and amplitude of

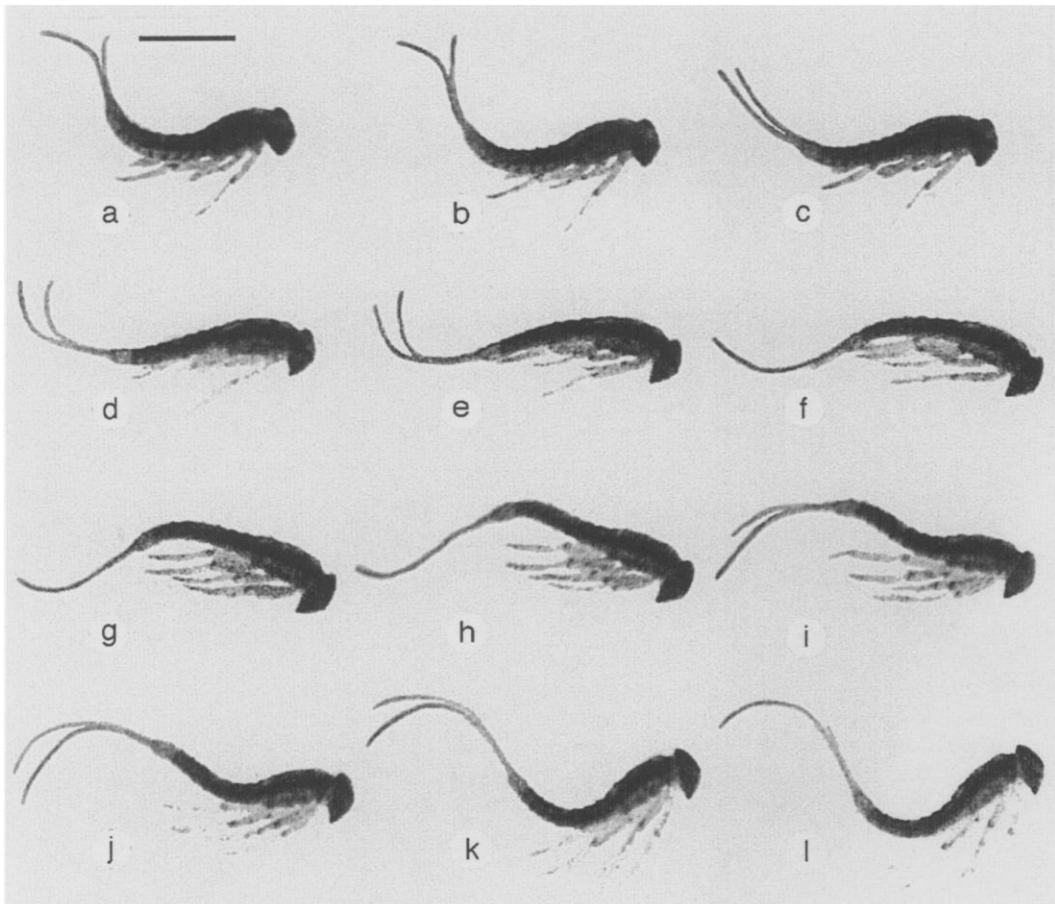


FIG. 6. Lateral view from a high-speed cine film sequence of a *Baetis tricaudatus* nymph (4.4 mm length) during 2 swimming sequences, showing abdominal flexion and leg positions. Time elapsed between images = 0.004 s. Scale bar = 2.0 mm.

abdominal oscillation appeared to affect swimming speed, results from this study were not statistically significant because of small sample size. Further observations are required before a general relationship between nymphal length, frequency, amplitude, and swimming speed can be described.

Average Swimming Speed.—Average speed (U_{av}) plotted against nymphal length (L) gave the relationship $U_{av} = 5.1L + 27.0$ ($r^2 = 0.016$, $p = 0.617$, $n = 18$), which was not a good predictor of the average swimming speed. A similar result was obtained for average Re , where the equation was $Re = 62.0L + 94.1$ ($r^2 = 0.15$, $p = 0.11$, $n=18$).

Instantaneous swimming speeds.—Instanta-

neous swimming was analyzed on 4 large nymphs that met the criteria described in the methods. Instantaneous speed was affected by abdominal position and angular speed. Minimum swimming speeds were observed as the nymphs were nearing completion of either a power or recovery stroke and the abdomen was either maximally flexed or deflexed (Fig. 6a, h). At this time angular speed of the abdomen was also at a minimum (Fig. 7a). The highest swimming speed was attained during the 1st cycle. Local maxima of speed and acceleration were reached when the abdomen approached its most linear position during the power and recovery strokes (Fig. 7a, b, c). Instantaneous Re was highest when the body approached maximum

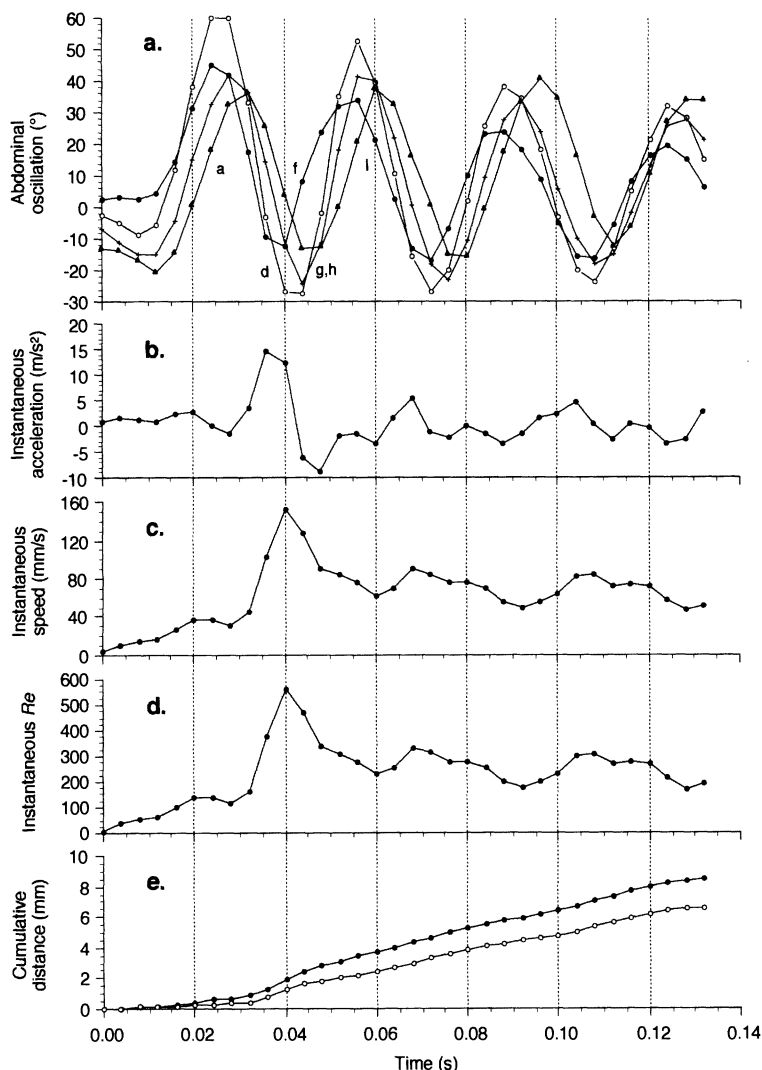


FIG. 7. Relationship among (a) abdominal oscillation ($\circ = At^{\circ}$, $\bullet = Ta^{\circ}$, $+ = A1^{\circ}$, $\triangle = A2^{\circ}$), (b) instantaneous acceleration, (c) speed, (d) instantaneous Reynolds number (Re), and (e) cumulative distance ($\bullet =$ total distance, $\circ =$ horizontal distance), in a *Baetis tricaudatus* nymph (4.4 mm long). Letters on (a) refer to film sequences in Fig. 6.

deflection during the power stroke and lowest as the nymph was nearing completion of the recovery stroke (Fig. 7d).

Transition of gait

Locomotory gait changed when nymphs were between ca 3.3–3.7 mm long (Fig. 8). Nymphs within this range exhibited either rowing or non-rowing swimming gaits, but the behavior

used by a particular individual was consistent. Three nymphs displayed an intermediate gait where the legs appeared to assume rowing-like motions, but the movement appeared more passive than rowing motions observed in smaller nymphs. Only 1 nymph in this size range met criteria for detailed analysis. The change in gait occurred between Re 60 and 90, which coincided with the transition from linear to exponential increase in speed (Fig. 8).

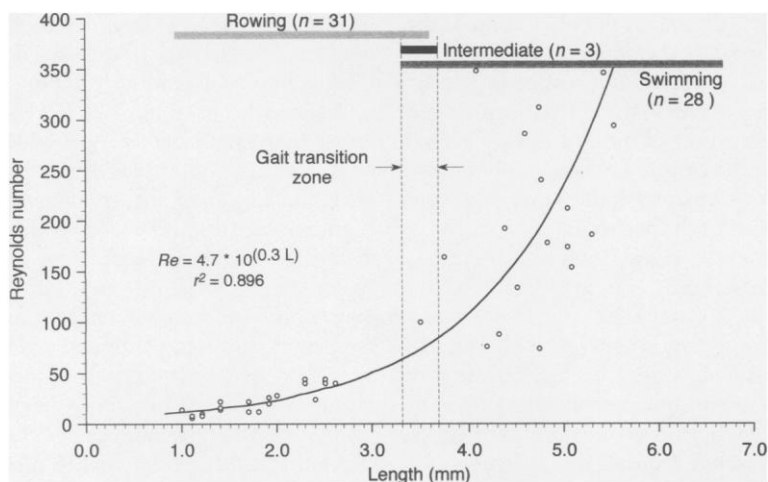


FIG. 8. Relationships of gait, gait transition zone, Reynolds number, and body length in *Baetis tricaudatus* nymphs. Numbers in parentheses are total observations of gaits, whereas points on the curve are quantified observations.

Discussion

Swimming gait of small *B. tricaudatus* nymphs (≤ 3.0 mm)

Small *B. tricaudatus* nymphs use dorso–ventral oscillations of the abdomen in conjunction with rowing movements of the legs to move in the water column. Contrary to observations made by Saita (1979), all abdominal oscillations occurred in the dorso–ventral plane (the cetacean model) as opposed to a lateral one (the picean model). Dorso–ventral oscillation is theoretically a more efficient means of generating thrust in *B. tricaudatus* nymphs because of the arrangement of their abdominal musculature and the dorso–ventral flattening of the abdomen (Craig 1990).

The use of dorso–ventral abdominal oscillations in concert with leg rowing in *Baetis* is a unique locomotory gait within the Insecta, but similar movements have been observed in *Cyclops* (Copepoda:Crustacea) and other copepods (e.g., Strickler 1975, Morris et al. 1985). These crustaceans and small *B. tricaudatus* nymphs are similar in size, shape, and flexibility of their corresponding abdominal sections. Therefore, it is not coincidental that these animals exhibit comparable swimming behaviors, because similar size places them in comparable hydrodynamic regimes (Webb and Weihs 1986).

Reynolds numbers taken from average veloc-

ities show that small *B. tricaudatus* nymphs are in a hydrodynamic environment where viscous forces predominate. Instantaneous Re frequently fell to 10, or lower, as the abdomen approached either the maximally flexed or deflexed position, and never rose above 30 (Fig. 4e). At such low Re , flows are reversible because of a lack of fluid circulating around an object. Propulsive methods of locomotion, which are inertial based, are not possible (Webb and Weihs 1986). Thus, organisms at low Re must use friction-based gaits to maintain the drag of the recovery stroke at a level lower than that experienced during the power stroke. If a power stroke equaled the recovery stroke in all aspects, an organism would experience virtually no net forward movement (Purcell 1977). This situation pertains, in part, to the jerky forward motion of the small nymphs observed here, where there is considerable backward movement during the recovery stroke (Fig. 4f).

Decreasing the effective area of the appendage during recovery, or moving it along a path near the body where the flow is slower, are 2 frequently adopted methods of lowering drag at low Re (Vogel 1994). These methods decrease the amount of water displaced during a recovery stroke relative to that of the power stroke. During the power stroke of a rowing *B. tricaudatus* nymph, the abdomen is positioned dorsal to the head and thorax and the legs are posi-

tioned ventrally, whereas at the beginning of the recovery stroke, both abdomen and legs are in the same plane, ventral to the rest of the body. This orientation decreases the frontal area exposed to the direction of motion during recovery. Drag would therefore be lowest when both the abdomen and legs are in the same plane because drag varies with the frontal area exposed to the flow ($D = 1/2 C_d \rho S U^2$ where D is drag, C_d is the drag coefficient, ρ is the density of the medium, S is the frontal area, and U is the velocity of the organism relative to the fluid). Nymphs extend their legs ventrally and laterally on the power stroke, but recover the legs ventrally in a somewhat flexed position, which localizes the projected frontal area. The ventral inclination of the head and thorax at the onset of the recovery stroke permits the legs to recover in the wake of the frontal portion of the body where the flow is slower, serving to minimize drag (Strickler 1975).

Decreases in speed occur twice during the swimming cycle of a nymph. These decreases can be attributed to the increase in exposed frontal area when the abdomen is in a flexed position and to the deceleration of the abdomen as it completes either a power or recovery stroke. The 1st component is a result of a greater area projected in the direction of the flow, which increases drag. As the surface area exposed increases, the forces countering forward movement also increase and the speed decreases. The 2nd component occurs as the abdomen changes its direction. When this change occurs, the speed of the abdomen is 0 and therefore does not contribute to the propulsion of the nymph.

Two localized peaks in acceleration occur shortly after the onset of either the power or recovery stroke. Another peak in acceleration, although ca 1/2 the magnitude of those previously described, occurs shortly after the legs (primarily prothoracic) begin moving towards the body (similar to the movement of a swimmer's arms when doing the breast-stroke). At any of these instances, the appendages involved are moving the most water and therefore produce high propulsive force (Fig. 4a, b).

The oscillation of the abdomen changes as nymphs grow. Rotation about A_1° , T_1° , A_1° , and A_2° are fairly synchronous in small nymphs (Fig. 4a), but slightly asynchronous in larger nymphs (Fig. 5). This change is likely a result of increasing flexibility as the abdomen becomes

longer. As the abdomen increases further in length it begins to undulate (Fig. 7a), rather than acting as a semi-stiff plate.

Frequently in nature, large organisms are faster than small ones (Vogel 1994). The results of this study conform to this general principle, with the larger of the small nymphs reaching higher velocities and therefore higher Re . However, high correlation in a linear relationship between length and Re suggests strict physical constraints on small *B. tricaudatus* by the fluid environment (Fig. 8). Speed also directly depends on frequency and amplitude of the oscillating appendages of body segments (Bainbridge 1958). Although our results support this dependence, the relationship between speed, frequency, amplitude, and length is not yet adequately established for *B. tricaudatus*.

Small *B. tricaudatus* nymphs exhibit burst movements consisting of an initial rowing-gait sequence followed by a temporary stop during which nymphs exhibit a splayed position in the water column, with the abdomen flexed dorsally and all legs somewhat extended. Burst swimming is energetically profitable (Weihs 1974) and is consistent with the field observations of swim-drift behaviors that are frequently adopted by streamlined mayflies (Peckarsky 1980).

*Swimming gait of large *B. tricaudatus* nymphs (≥4.0 mm)*

Large nymphs used only abdominal oscillations to swim. As the abdomen oscillated, the head and thorax rotated as well. This rotation likely contributes to momentum balance while swimming (Fish and Hui 1991). Physical principles of locomotion dictate that at Re above 200–500 inertial-based propulsors are efficient means of transportation (Webb and Weihs 1986, Daniel and Webb 1987). At higher Re , a streamlined body form is desirable because it delays separation of the boundary layer, decreases the wake at the trailing end (thereby decreasing pressure drag), and reduces the added mass coefficient during fast starts (Craig 1990).

Amplitude of abdominal oscillations was lower in large nymphs (Figs 6, 7a) compared to small nymphs (Figs 2, 3, 4a). Maximum speeds and accelerations were achieved when nymphs were in the most linear position and parallel to the direction of motion. These maxima are likely the combined result of high acceleration and an-

gular speed of the abdomen at these times and because the projected frontal area was smallest.

Body length was not a good predictor of speed in large nymphs (Fig. 8), which suggests that they are less rigidly confined by properties of their hydrodynamic regime. Large nymphs, although capable of high accelerations and swimming speeds, may not always accelerate rapidly or swim at their maximum speed. The stimulus strength that elicits swimming behavior, be it spontaneously generated or to escape from a predator, is possibly the factor that determines magnitude of swimming response.

Transition of gait

At the point where nymphs change gait there is an exponential increase in speed (Fig. 8). This change in speed occurs at a transition zone where viscous forces decrease and inertial forces dominate and, as Re approach 100, vortex formation commences (Behan 1997).

Few of the nymphs observed fell in the transition zone where the gait change took place. However, based on limited observations of nymphs exhibiting these intermediate gaits, the transition from rowing to swimming, although gradual, occurs over a small size range. As nymphs became capable of swimming at higher speeds, the movements of the legs became more passive and were gradually held closer to the body as would be dictated by a thinner boundary layer surrounding a fast-moving nymph (Craig 1990).

Implications of gait transition

Outcomes of predator-prey interactions depend on the behavior of the participants, which are in turn influenced by their physical capabilities (Webb 1986), so there are ecological implications in the 2 gaits used by *Baetis* nymphs. Scrimgeour et al. (1994) have shown that *B. tricaudatus* nymphs display risk-adjustment strategies in predator-prey interactions involving longnose dace (*Rhinichthys cataractae*). Risk-adjusting occurred in high- and low-food treatments and depended on length of nymph involved in the interaction. Large nymphs delayed flight initiation upon predator detection in high-food regimes, whereas small nymphs fled once they detected the dace in both high- or low-food treatments. Although no mechanism for size-de-

pendent risk adjustment was determined, Scrimgeour et al. (1994) suggested that the speed at which mayfly nymphs swim away from an approaching predator might explain the size-specific flexibility in drift initiation distances displayed by *Baetis* nymphs. The findings from our study better explain their results. Small nymphs restricted in speed by low Re should have longer flight-initiation distance than large nymphs, which, because of their size, can push through that restriction.

This transition has ontogenetic implications. *Baetis* nymphs may show disproportionate increases in relative length of abdomen to thorax and legs at the point in their development where they can pass rapidly through the transition zone. This point of development would have the effect of rapidly increasing the linear function in Re and would concomitantly provide volume for more muscle to achieve higher speed (Daniel and Webb 1987). There may be other changes as well. Some Ephemeroptera nymphs are known to have an unusual muscle configuration that is apparently involved in achieving fast starts (Craig 1990). It would be interesting to investigate allometry of growth and muscle structure in *Baetis* nymphs over the transition zone of gaits.

Acknowledgements

We thank G. J. Scrimgeour and 2 anonymous reviewers for constructive comments. The study was supported by a Natural Sciences and Engineering Research Council of Canada grant OGP-5753 to D. A. C.

Literature Cited

- ARCHER, S. D., AND I. A. JOHNSTON. 1989. Kinematics of labriform and subcarangiform swimming in the Antarctic fish *Notothenia neglecta*. *Journal of Experimental Biology* 143:195–210.
- BAINBRIDGE, R. 1958. The speed of swimming of fish as related to size and to the frequency and amplitude of the tail beat. *Journal of Experimental Biology* 35:109–133.
- BATTY, R. S. 1981. Locomotion of plaice larvae. *Symposia of the Zoological Society of London* 48:53–69.
- BATTY, R. S. 1984. Development of swimming movements and musculature of larval herring (*Clupea harengus*). *Journal of Experimental Biology* 110: 217–229.

- BEHAN, A. 1997. Advanced engineering thermodynamics. 2nd edition. John Wiley and Sons, Toronto.
- CRAIG, D. A. 1990. Behavioral hydrodynamics of *Cloeon dipterum* larvae (Ephemeroptera: Baetidae). Journal of the North American Benthological Society 9:346–357.
- CULP, J. M., AND G. J. SCRIMGEOUR. 1993. Size-dependent diel foraging periodicity of a mayfly grazer in streams with and without fish. Oikos 68:242–250.
- DANIEL, T. L., AND P. W. WEBB. 1987. Physical determinants of locomotion. Pages 343–369 in P. Dejours, L. Bolis, C. R. Taylor, and E. R. Weibel (editors). Comparative physiology: life in water and on land. Fidia Research Series 9. Liviana Press, Padova.
- FISH, F. E., AND C. A. HUI. 1991. Dolphin swimming—a review. Mammal Review 21:181–195.
- HUNTER, J. R. 1972. Swimming and feeding behavior of larval anchovy *Engraulis mordax*. US National Marine Fisheries Service Fishery Bulletin 70:821–838.
- HYNES, H. B. N. 1970. The ecology of running waters. University of Toronto Press, Toronto.
- MORRIS, M. J., G. GUST, AND J. J. TORRES. 1985. Propulsion efficiency and cost of transport for copepods: a hydromechanical model of crustacean swimming. Marine Biology 86:283–295.
- NACHTIGALL, W. 1974. Locomotion: mechanics and hydrodynamics of swimming in aquatic insects. Pages 381–432 in M. Rockstein (editor). The physiology of Insecta, Volume 3. 2nd edition. Academic Press, New York.
- NEEDHAM, J. G., AND J. T. LLOYD. 1916. The life of inland waters. Comstock Publishing Company, Ithaca, New York.
- PECKARSKY, B. L. 1980. Predator-prey interactions between stoneflies and mayflies: behavioral observations. Ecology 61:932–943.
- PURCELL, E. M. 1977. Life at low Reynolds number. American Journal of Physiology 45:3–11.
- SAITA, A. 1979. Analysis of abdominal movements in nymphal Ephemeroptera by means of high-speed cinematography. Pages 279–292 in Proceedings of the 2nd International Conference on Ephemeroptera (1975), Państwowe Wydawnictwo Naukowe, Warsaw-Kraków.
- SCRIMGEOUR, G. J., J. M. CULP, AND F. J. WRONA. 1994. Feeding while avoiding predators: evidence for a size-specific trade-off by a lotic mayfly. Journal of the North American Benthological Society 13: 368–378.
- STATZNER, B. 1988. Growth and Reynolds number of lotic macroinvertebrates: a problem for adaptation of shape to drag. Oikos 51:84–87.
- STRICKLER, J. R. 1975. Swimming of planktonic *Cyclops* species (Copepoda, Crustacea): pattern, movements and their control. Pages 599–613 in T. Y.-T. Wu, C. J. Brokaw, and C. Brennen (editors). Swimming and flying in nature. Volume 2. Plenum Press, New York.
- VOGEL, S. 1994. Life in moving fluids: the physical biology of flow. 2nd edition. Princeton University Press, Princeton, New Jersey.
- WEBB, P. W. 1986. Effect of body form and response threshold on the vulnerability of four species of teleost prey attacked by largemouth bass (*Micropterus salmoides*). Canadian Journal of Fisheries and Aquatic Sciences 43:763–771.
- WEBB, P. W. 1994. The biology of fish swimming. Pages 45–62 in L. Maddock, Q. Bone, and J. M. V. Rayner (editors). Mechanics and physiology of animal swimming. Cambridge University Press, Cambridge, UK.
- WEBB, P. W., AND D. WEIHS. 1986. Functional locomotor morphology of early life history stages of fishes. Transactions of the American Fisheries Society 115:115–127.
- WEIHS, D. 1974. Energetic advantages of burst swimming of fish. Journal of Theoretical Biology 48: 215–229.
- WEIHS, D. 1980. Energetic significance of changes in swimming modes during growth of anchovy larvae, *Engraulis mordax*. US National Marine Fisheries Service Fishery Bulletin 77:597–604.

Received: 8 June 1998

Accepted: 10 December 1998